Synthesis and Solution Conformational Analysis of 2,3-Anhydro-3-*C*-[(1*R*)-2,6-anhydro-1-deoxy-1-fluoro-D-*glycero*-D-*gulo*-heptitol-1-*C*-yl]-*β*-D-*gulo*-furanose: First Example of a Monofluoromethylene-Linked *C*-Disaccharide

Jesús Jiménez-Barbero,* Raynald Demange, Kurt Schenk, and Pierre Vogel*

Section de Chimie, Université de Lausanne, BCH, CH-1015 Lausanne-Dorigny, Switzerland, Instituto de Química Orgánica, CSIC, Juan de la Cierva 3, E 28006 Madrid, Spain, and Institut de Cristallographie de l'Université, BSP, CH-1015-Lausanne-Dorigny, Switzerland

pierre.vogel@ico.unil.ch

Received March 6, 2001

Condensation of 2,3,4,6-tetra-*O*-benzyl-*β*-D-glucopyranosylcarbaldehyde with isolevoglucosenone induced by Et_2AlI, followed by epoxidation, gave an aldol that was fluorinated into a monofluoromethylene *C*-glucopyranoside that was converted into the title *C*-disaccharide **1**. Its conformational behavior in water has been studied by using a combination of NMR spectroscopy (*J* and NOE data) and molecular mechanics calculations.

Introduction

The quest for glycosidase and glycosyl transferase inhibitors, as well as for stable glycomimetics, has led to different groups of oligosaccharide analogues with the glycosidic and endocyclic oxygens substituted by other atoms.[1] Thus, carbon-, thio-, and imino-linked glycosides, carbasugars, and other derivatives have been employed, with different degrees of success.[2,3] For these pseudosaccharides to be biologically useful, one of the requirements probably concerns that their conformational behavior should be analogous to that of the natural compound, to minimize the entropic costs of the recognition process with the receptor.[4] It should be stressed that, in principle, the substitution of the exo- or endocyclic oxygens by other atoms will result in a change in both the size and/or the electronic properties of the glycosidic linkage, particularly in the conformational anomeric effects.[5] Therefore, it is relevant to determine how the three-dimensional structures of the synthetically prepared derivatives are affected by such modifications, in relation to those of the corresponding *O*-glycosides. In this context, we have recently reported that for the *C*-glycosyl, *S*-glycosyl, and carba analogues of lactose,[6] in the absence of the stereoelectronic stabilization provided by the anomeric effect, conformations which are not consistent with the *exo-anomeric-syn* disposition can be adopted (4−50%), which depends on the strength of 1,3-type syn-diaxial interactions and the particular bond distance and angle values. Regarding the recognition of these analogues by proteins and enzymes, we have also reported that thiocellobiose is bound by *Streptomyces* sp. *β*-glucosidase in the conformation usually found for regular *O*-glycosides (syn-Φ,Ψ).[7] However, we also have described that the *C*-glycosyl analogue of lactose is bound by *Escherichia coli* *β*-galactosidase in an unusual high energy conformation.[8] Moreover, this derivative, *C*-lactose, is recognized by two lectins, namely, ricin-B and galectin-1, in other distinct conformations.[9,10] These results have prompted us to extend our studies to determine which is the degree of similarity between other sugars and their analogues, with different glycosidic linkages, in the free and in the protein-bound state.[11]

On this basis, we report here on the synthesis and conformational study of a new *C*-disaccharide, **1**, in which *β*-D-glucopyranose is linked by a monofluoromethylene bridge at position C3 of 2,3-anhydro-D-gulofuranose. The conformation analysis of **1** will use a combination of NMR spectroscopy and molecular mechanics calculations.[12,13] Compound **1** represents the first example of a new class

(1) (a) Gabius, H. J.; Gabius, S. In *Glycosciences: Status and Perspectives*; Chapman & Hall: London, 1997. (b) *Chemistry of C-glycosides*; Levy, W., Chang, D., Eds.; Elsevier: Cambridge, 1995. (c) *C-Glycoside synthesis*; Postema, M. D. H., Ed.; CRC Press: Boca Raton, FL, 1995. (d) Driguez, H. *Top. Curr. Chem.* **1997**, *187*, 85. (e) Andrews, J. S.; Pinto, B. M. *Carbohydr. Res.* **1995**, *270*, 51. (f) Yuasa, H.; Hashimoto, H. *Rev. Heteroat. Chem.* **1999**, *19*, 35.

(2) (a) Johns, B. A.; Pan, Y. T.; Elbein, A. D.; Johnson, C. R. *J. Am. Chem. Soc.* **1997**, *119*, 4856. (b) Gabius, H. J., Sinowatz, F., Eds. Special volume on glycosciences. *Acta Anat.* **1998**, *161*, 1.

(3) Ogawa, S.; Hirai, K.; Odagiri, T.; Matsunaga, N.; Yamazaki, T. A.; Nakajima, A. *Eur. J. Org. Chem.* **1936**, *1*, 1099, and references therein.

(4) Searle, M. S.; Williams, D. H. *J. Am. Chem. Soc.* **1992**, *114*, 10690.

(5) (a) Asensio, J. L.; Cañada, F. J.; García, A.; Murillo, M. T.; Fernández-Mayoralas, A.; Johns, B. A.; Kozak, J.; Zhu, Z.; Johnson, C. R.; Jiménez-Barbero, J. *J. Am. Chem. Soc.* **1999**, *121*, 11318. (b) Asensio, J. L.; Cañada, F. J.; Kahn, N. Mootoo, D. A.; Jiménez-Barbero, J. *Chem. Eur. J.* **2000**, *6*, 1035.

(6) Montero, E.; García, A.; Asensio, J. L.; Hirai, K.; Ogawa, S.; Santoyo-González, F.; Cañada, F. J.; Jiménez-Barbero, J. *Eur. J. Org. Chem.* **2000**, 1945.

(7) Montero, E.; Vallmitjana, M.; Perez-Pons, J. A.; Querol, E.; Jiménez-Barbero, J.; Cañada, F. J. *FEBS Lett.* **1998**, *421*, 243.

(8) Espinosa, J. F.; Montero, E.; Vian, A.; Garcia, J. L.; Dietrich, H.; Martín-Lomas, M.; Schmidt, R. R.; Imberty, A.; Cañada, F. J.; Jiménez-Barbero, J. *J. Am. Chem. Soc.* **1998**, *120*, 10862.

(9) (a) Espinosa, J. F.; Cañada, F. J.; Asensio, J. L.; Dietrich, H.; Martín-Lomas, M. Schmidt, R. R.; Jiménez-Barbero, J. *Angew. Chem., Int. Ed. Engl.* **1996**, *35*, 303. (b) Espinosa, J. F.; Cañada, F. J.; Asensio, J. L.; Martín-Pastor, M.; Dietrich, H.; Martín-Lomas, M.; Schmidt, R. R.; Jiménez-Barbero, J. *J. Am. Chem. Soc.* **1996**, *118*, 10862.

(10) Asensio, J. L.; Espinosa, J. F.; Dietrich, H.; Cañada, F. J.; Schmidt, R. R.; Martín-Lomas, M.; André, S.; Gabius, H. J.; Jiménez-Barbero, J. *J. Am. Chem. Soc.* **1999**, *121*, 8995.

(11) Ravishankar, R.; Surolia, A.; Vijayan, M.; Lim, S.; Kishi, Y. *J. Am. Chem. Soc.* **1998**, *120*, 11297.

(12) (a) Peters, T.; Pinto, B. M. *Curr. Opin. Struct. Biol.* **1996**, *6*, 710. (b) Imberty, A. *Curr. Opin. Struct. Biol.* **1997**, *7*, 617. (c) Jiménez-Barbero, J.; Asensio, J. L.; Cañada, J.; Poveda, A. *Curr. Opin. Struct. Biol.* **1999**, *9*, 549.

10.1021/jo0102462 CCC: $20.00
Published on Web 07/04/2001

Scheme 1

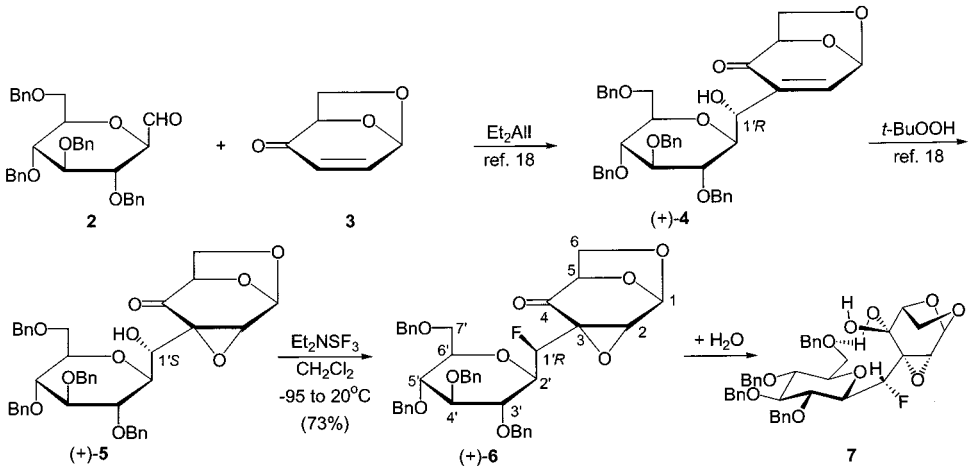

of *C*-disaccharides. The few fluorinated *C*-disaccharides reported so far are difluoromethylene-linked *C*-furanosides.[14,15] As we shall see, the monosubstitution of the methylene linker in *β*-*C*-glucopyranoside allows for unusual conformations to exist in equilibrium with "normal" conformations of the *C*-glycosides.

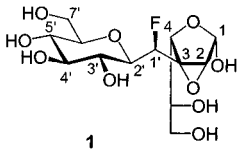

1

Results and Discussion

Synthesis. The synthesis of the fluoromethylene-linked *C*-disaccharide **1** starts with a Baylis−Hillmann type of condensation of the *β*-D-glucopyranose-derived carbaldehyde **2**[16] with isolevoglucosenone **3**[17] induced by Et_2AlI. The enone (+)-**4** so obtained is epoxidized stereospecifically into (+)-**5**.[18] Fluorination of (+)-**5** with DAST (Et_2NSF_3)[19] in CH_2Cl_2 afforded (+)-**6** in 73% yield (Scheme 1). The stucture of (+)-**6** was established unambiguously by single-crystal X-ray radiocrystallography of its hydrate **7** obtained when crystalline (+)-**6** was left in the air. Interestingly, **7** adopts about its C1′−C2′ bond an unusual conformation. Indeed, the O−C2′ and C1′−C3 bonds of **7** are nearly synperiplanar (dihedral angle: +8.49(26)° and −6.47(27)° for the two forms found in the monocrystal). The quasi eclipsing of bonds O−C2′ and C1′−C3 of **7** is probably due to hydrogen bonding involving one of the 4-hydroxy groups and the ethereal oxygen center at C7′ of the *C*-*β*-D-glucopyranoside unit of **7**. The structure of **7** confirms an S_N2-type displacement (no intervention of participating groups in the heterolytic process) for the fluorination of aldol (+)-**5** into the *β*-fluoroketone (+)-**6**. The (1′*S*) configuration of the hydroxymethylene linker of *C*-disaccharide (+)-**5** has been established unambiguously by conversion of (+)-**5** into 1,6:2,3-dianhydro-3-*C*-[(1*S*)-2,6-anhydro-D-*glycero*-D-*gulo*-heptitol-1-*C*-yl]-*β*-D-*gulo*-pyranose-1′,4-acetonide.[18]

Reduction of ketone (+)-**6** with $NaBH_4$ in MeOH was highly stereoselective and gave (+)-**8** quantitatively. Debenzylation of (+)-**8** with metallic sodium in ammonia[20] afforded the fully deprotected dianhydro-*C*-disaccharide (+)-**9** in 95% yield. Peracetylation under standard conditions (Ac_2O, pyridine, DMAP) gave the pentaacetate (+)-**10** (96%) that reacted with trifluoroacetic acid in acetic anhydride, giving rise to the 2,3-anhydro-D-gulose derivative (+)-**11** in 73% yield. The structure of (+)-**11** was deduced from its coupling constant ^3J(H-1,H-2) = 3.0 Hz.[21] Ammonolysis of (+)-**11** in MeOH liberated **1** in 77% yield. Its ^{1}H NMR spectrum showed a 7:1 mixture of the α-furanose form **1** and α-pyranose form **12** (Scheme 2).

Molecular Mechanics and Dynamics Calculations. *C*-Disaccharide **1** shows two torsional degrees of freedom (Φ, Ψ) for the glycosidic linkage and two more for the corresponding lateral chains. Therefore, in a first step, the population of the different staggered rotamers around the Φ/Ψ linkages was estimated (Figure 1) by using the MM3* force field.[22] Glycosidic torsion angles are defined as Φ (H−C2′/C1′−C3) (rotamers about C2′−C1′ bond), Ψ (C2′−C1′/C3−C4) (rotamers about C1′−C3 bond), *ω*1 as dihedral angle (O4−C4/C5−C6), *ω*2 as (C4−C5/C6−O6), and *ω*3 as (C5′−C6′/C7′−O). The results are shown in Table 1.

For Ψ and $\omega_{2,3}$, the rotamers are defined as *g*+ (60°), *g*− (−60°), and *anti* (180°), while for Φ, conformers in agreement with the *exo*-anomeric orientation (Φ ca. +60°) and in disagreement (Φ ca. −60°) are denoted as *exo* and

(13) A general survey of conformation of carbohydrates and analogues is presented in the following: French, A. D.; Brady, J. W. *Computer Modelling of Carbohydrate Molecules*; American Chemical Society: Washington, DC, 1990. For carba sugars, besides ref 6, see: (a) Duus, J. O.; Bock, K.; Ogawa, S. *Carbohydr. Res.* **1994**, *252*, 1. (b) Duus, J. O.; Guzmán, J. F.; Bock, K.; Ogawa, S.; Yokoi, F. *Carbohydr. Res.* **1991**, *209*, 51. (c) Bock, K.; Guzmán, J. F.; Ogawa, S. *Carbohydr. Res.* **1988**, *174*, 354. (d) Bock, K.; Ogawa, S.; Orihara, M. *Carbohydr. Res.* **1989**, *191*, 357.

(14) (a) Motherwell, W. B.; Ross, B. C.; Tozer, M. J. *Synlett* **1989**, 68. (b) Herpin, T. F.; Motherwell, W. B.; Tozer, M. J. *Tetrahedron: Asymmetry* **1994**, *5*, 2269.

(15) (a) Kovensky, J.; Burrieza, D.; Colliou, V.; Fernández-Cirelli, A.; Sinay, P. *J. Carbohydr. Chem.* **2000**, *19*, 1. (b) Plantier-Royon, R.; Portella, C. *Carbohydr. Res.* **2000**, *327*, 119.

(16) (a) Wang, Y.; Babirad, S. A.; Kishi, Y. *J. Org. Chem.* **1992**, *57*, 468. (b) Haneda, T.; Kim, S. H.; Kishi, Y. *J. Org. Chem.* **1992**, *57*, 490.

(17) Horton, D.; Roski, J. P.; Norris, P. *J. Org. Chem.* **1996**, *61*, 3783.

(18) Zhu, Y.-H.; Demange, R.; Vogel, P. *Tetrahedron: Asymmetry* **2000**, *11*, 263.

(19) Shellhamer, D. F.; Briggs, A. A.; Miller, B. M.; Prince, J. M.; Scott, D. H.; Heasley, V. L. *J. Chem. Soc., Perkin Trans. 2* **1996**, 973.

(20) (a) Cheney, L. C.; Piening, J. R. *J. Am. Chem. Soc.* **1945**, *67*, 2252. (b) Procter, G.; Genin, D.; Challenger, S. *Carbohydr. Res.* **1990**, *202*, 81.

(21) (a) Buss, D. H.; Hough, L.; Hall, L. D.; Manville, J. F. *Tetrahedron* **1965**, *21*, 69. (b) Chmielewski, M.; Mieczkowski, J.; Priebe, W.; Zamojski, A. *Tetrahedron* **1978**, *34*, 3325. (c) Abdel-Malik, M. M.; Peng, Q.-J.; Perlin, A. S. *Carbohydr. Res.* **1987**, *159*, 11.

Scheme 2

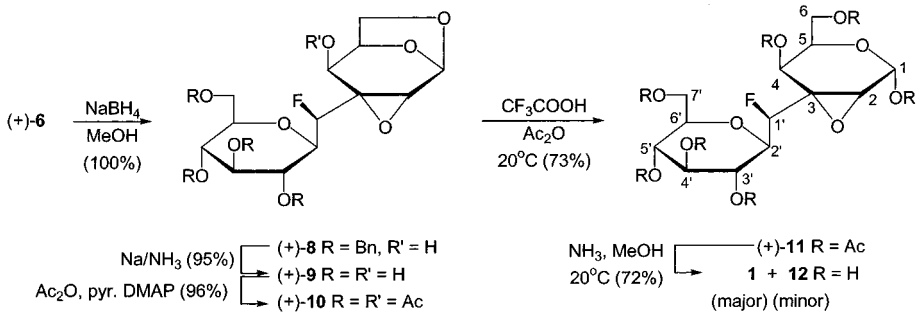

Table 1. Summary of the Molecular Mechanics Calculations Carried out for 1 (MM3*, MACROMODEL)

conformer (Φ, ψ)	Δ*E*, kJ mol^{-1}	relative populations	$J_{1',2'}$ (hertz)	H-2′, H-4	H-2′, H-2	H-3′, H-4′	H-3′, H-2	H-1′, H-3′	H-1′, H-2	H-1′, H-4
anti-Φ/*g*− 178, −49	0.0	42.5[b]	2.8	4.1	4.5	*2.7*	***2.5***	3.1	*2.8*	4.0
anti-Φ/*anti* 180, 161	2.4	16.2[b]	2.7	5.0	4.2	4.7	4.2	3.1	4.0	*2.9*
exo-Φ/*anti* 61, 165	2.8	13.9[b]	9.6	4.7	***2.1***	5.4	5.3	***2.5***	4.0	*3.0*
exo-Φ/*g*− 60, −51	1.4	24.3[b]	9.6	***2.4***	4.2	5.1	4.4	***2.5***	2.8	4.2
non-*exo*-Φ/*g*+ −40, 156	8.9	1.2	0.7	4.9	2.9	5.0	5.2	3.7	2.9	2.7
non-*exo*-Φ/*anti* −40, 156	15.9	0.1	0.4	4.7	4.1	5.3	3.1	3.7	4.0	2.8
exo-Φ/*g*+ 49, 49	10.0	0.8	9.6	3.6	4.9	4.0	6.6	*2.6*	3.8	*2.9*
anti-Φ/g− 58	9.9	0.8	1.0	4.5	4.9	***2.3***	5.1	*2.9*	*2.8*	*2.9*
non-*exo*-Φ/*g*− −26, −59	14.3	0.2	0.6	*2.8*	2.8	4.1	5.4	3.6	2.8	4.0
ensemble average		100.0	5.4	*3.0*	*2.9*	*3.1*	*2.9*	*2.6*	*3.0*	*3.0*

[a] Expected coupling constants (*J* in hertz) and expected distances (*r*, Å) for every conformer are also given. Distances smaller than 2.5 Å that correspond to strong NOEs are in bold type. Distances smaller than 3 Å are detected experimentally and are in italic type. [b] See Figure 1 for representations of these conformations.

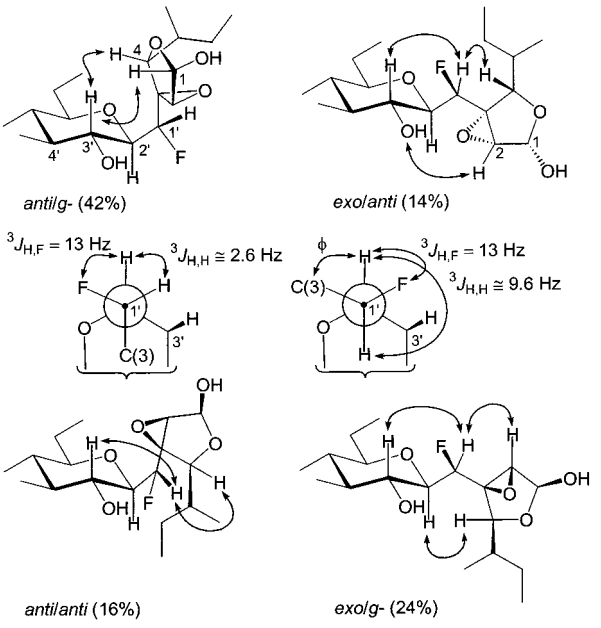

Figure 1. Representation of major conformers of **1** and significant vicinal coupling constants.

non-*exo*, respectively. For ω_1, the rotamers are dubbed *gg*, *gt*, and *tg*. The first letter *g* or *t* considers the torsion O4−C4/C5−C6 and the second one C3−C4/C5−C6.

From the calculated energy values (Table 1), it is obvious that only four conformers (*anti*-Φ/*a*, *anti*-Φ/*g*−, *exo-syn*-Φ/*a*, and *exo-syn*-Φ/*g*−) have appreciable population according to a Boltzmann function (Table 1). Therefore, two rotamers around Φ (*anti*-Φ (60%) and *syn-exo*-Φ (39%)) and two around Ψ are favored (*g*− (67%) and *anti* (30%)). Nevertheless, it can be observed that, although destabilized by more than 2.5 kcal/mol, non-*exo* conformers around Φ were local minima (ca. 2% population), as well as the *exo* and *anti* conformers. This result is in contrast to usual *O*-glycosides, for which these non-*exo* conformers are not local minima. In fact, molecular mechanics calculations carried out for the putative *O*-analogue (**13**) of **1** confirmed this point, and the non-*exo* conformers converged to the corresponding *exo-syn* geometries.

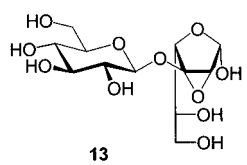

13

For the torsional Φ/Ψ combinations, the four conformers are within an energy range of only 0.5 kcal/mol. Therefore, the calculations predict a high amount of conformational freedom. *exo*-Anomeric *anti* and *syn* conformers in Φ, together with *anti* or *g*− conformers around Ψ, are predicted to be the most stable combina-

Table 2. Summary of Experimental ^{1}H NMR (500 MHz) Chemical Shifts (δ, ppm), Coupling Constants (J in hertz), and NOEs (%) for a Solution of 1 in D_2O at 25 °C

proton	δ_H (ppm)	J (hertz)	NOE with
H-1	5.43 (5.49)[a]	1.7	H-2
H-2	3.88 (3.78)	1.7	H-1′
H-4	4.58 (4.22)	1.9	2′S H-2′ (s)[b] H-1′ (s)
H-5	4.19	5.0 (5.0)[a]	
H-6a	3.67	-	
H-6b	3.68	-	
H-1′	4.95 (5.18)	4.0	H-4 (w) H-2 (s), H-2′ (s) H-3′ (s)
H-2′	3.85	4.0 (8.5)	H-4 (s)
H-3′	3.53	8.6	H-1′, H-4′ (s), H-6 (s)
H-4′	3.49	8.8	
H-5′	3.40	8.7	
H-6′	3.44	2.8 (5.5)	
H-7′a	3.74	-	
H-7′b	3.75	-	

[a] Values in parentheses are those observed for the minor pyranose **12** at equilibrium with **1**. [b] s = strong NOE, w = weak NOE.

tions. Minor populations of non-*exo* conformers around Φ (1−2%) and *g*+ (3%) conformers around Ψ are predicted. Regarding ω_1, similar energy values were found for the three rotamers for basically all Φ/Ψ combinations, with preference for the *gt* and *gg* rotamers.

Additional information on the conformational stability of the different minima was obtained from MD simulations with the MM3* force field using the continuum GB/SA (generalized Born solvent-accessible surface area) solvent model for water.[23] Independently from the starting minimum, the calculated trajectories showed several interconversions among the different regions and presented a clear resemblance to the conformer populations described above (Figure 1). In particular, *exo*-anomeric and *anti* conformers were major for Φ, and no excursions to non-*exo*-anomeric regions were detected (data not shown). Ψ angle is always between within the *g*− and *anti* regions. Interconversions around $\omega_1-\omega_3$ were very frequently found, in agreement with the molecular mechanics energy values and the experimental *J* values (see below).

NMR Studies. The validity of the predictions obtained through the molecular mechanics calculations was tested using ^{1}H NMR measurements, especially NOE and *J* values. In a first step, the assignment of the resonances was made through a combination of COSY, HSQC, and TOCSY experiments at 500 MHz. The results are shown in Table 2. The proton−proton coupling constants ($J_{4,5}$ = 1.9, $J_{5,6a}$ = 5.0, $J_{5,6b}$ = 5.0 Hz) for the furanose lateral chain and for Φ torsion angle ($J_{1',2'}$ = 4.0 Hz) agree with a conformational equilibrium among several conformers. Expected couplings were calculated from the molecular mechanics-based conformational distribution using the Altona modification of the Karplus equation.[24] The expected *J* values were calculated for each conformer, weighted according to its particular population, and averaged, producing, in all cases, a satisfactory agreement with the experimental values. The torsion angle around the C4−C5 linkage should be in the vicinity of the *gt* and *gg* conformers, since the corresponding coupling constant ($J_{4,5}$ < 2 Hz) agrees with the values predicted for both conformers (2.0−2.8 Hz). A similar agreement is produced for the C5−C6 linkage Therefore, the MM3* values seem to correctly reproduce the conformational behavior around these torsions.

The key conformational information around the Φ angle was obtained from the *J* (4.0 Hz) value and NOE experiments. The $^3J_{H,H}$ value is between those expected for the *exo*-anomeric *anti* (2.5 Hz) and *exo* (9.8 Hz) geometries (Figure 1), showing evidence of the conformational equilibrium around Φ, with a higher proportion of *anti* geometries (ca. 75:25) than that predicted from MM3* calculations[25] (60:38). In all four major conformers calculated for **1** (Figure 1), the dihedral angle between H−C2′ and C1′−F approaches 60°. For deoxyfluoropyranosides, the $^3J_{H,F}$ coupling constant in such a geometry is expected to vary between 12 and 15 Hz.[26] The value of 13 Hz measured for ^3J(H−C2′, F−C1′) of **1** is in perfect agreement with the predictions given by our molecular mechanics calculations and corroborates the other ^{1}H NMR data. Additional information came from NOEs. A close inspection to the 3D models for the basic *exo*-anomeric and non-*exo*-anomeric conformations around this linkage indicated that there are exclusive[27] interresidue NOEs that unequivocally characterize the different conformations. Thus, 2D-NOESY and 1D-DPFGSE NOESY[28] spectra were acquired (see Supporting Information).

The *exo*/*g*− conformation is characterized by short H4−H2′ distances of 2.4 Å. In addition, H-1′/H-3′ and H-1′/H-2 are 2.5 and 2.8 Å, respectively. The *exo*/*anti* conformer is characterized by a short H-2′/H-2 distance (only 2.1 Å). H-1′/H-3′ and H-1′/H-4 are 2.5 and 3.0 Å, respectively. The *anti*/*g*− conformer places H-3′ and H-4 and H-3′ and H-2 at 2.7 and 2.5 Å, respectively, while the H-1′ of the C linker is 2.8 Å apart of H-2. No exclusive NOE does exist for the *anti*/*anti* conformer. Therefore, the unambiguous presence of either conformer can be detected by focusing on the existence of these. Indeed, this is the case. Many of these NOEs are seen in water solution. Indeed, strong to medium H-4/H-2′, H-4/H-3′, H-1′/H-3′, and H-1′/H-2 NOEs may be observed unambiguously, indicating the presence of a major conformational equilibrium around both glycosidic linkages. On top with this, a weak NOE between H-1′/H-4 proton pairs is also observed. Therefore, these data indicate that the expected *syn exo*-anomeric conformer is in equilibrium in solution with the *anti*-Φ conformer, in agreement with

(22) The MM3* force field (Allinger, N. L.; Yuh, Y. H.; Lii, J. H. *J. Am. Chem. Soc.* **1989**, *111*, 8551) implemented in MACROMODEL (Mohamadi, F.; Richards, N. G. J.; Guida, W. C.; Liskamp, R.; Caufield, C.; Chang, G.; Hendrickson, T.; Still, W. C. *J. Comput. Chem.* **1990**, *11*, 440) differs of the regular MM3 force field in the treatment of the electrostatic term since it uses charge−charge instead of dipole−dipole interactions. The MM3* force field was used since it has provided a satisfactory agreement between experimental and theoretical data for a variety of saccharides and carba sugars.[6] For specific cases, see: (a) Espinosa, J. F.; Dietrich, H. M.; Martín-Lomas, M.; Schmidt, R. R.; Jiménez-Barbero, J. *Tetrahedron Lett* **1996**, *37*, 1467. (b) Martín-Pastor, M.; Espinosa, J. F.; Asensio, J. L.; Jimenez-Barbero, J. *Carbohydr. Res.* **1997**, *298*, 15.

(23) Still, W. C.; Tempczyk, A.; Hawley, R. C.; Hendrickson, T. *J. Am. Chem. Soc.* **1990**, *112*, 6127.

(24) Haasnoot, C. A. G.; de Leeuw, F. A. A. M.; Altona, C. *Tetrahedron*, **1980**, *36*, 2783.

(25) Perez, S.; Imberty, A.; Engelsen, S.; Gruza, J.; Mazeau, K.; Jimenez-Barbero, J.; Poveda, A.; Espinosa, J. F. *Carbohydr. Res.* **1998**, *314*, 141.

(26) See, for example: (a) San Fabián, J.; Guilleme, J.; Díez, E. *J. Magn. Reson.* **1998**, *133*, 255. (b) Thibaudeau, C.; Plavec, J.; Chattopadhyaya, J. *J. Org. Chem.* **1998**, *63*, 4967. (c) San Fabián, J.; Guilleme, J. *Chem. Phys.* **1996**, *206*, 325. (d) Emsley, J. W.; Phillips, L.; Wray, V. *Prog. NMR Spectrosc.* **1976**, *10*, 83.

(27) Dabrowski, J.; Kozar, T.; Grosskurth, H.; Nifant'ev, N. E. *J. Am. Chem. Soc.* **1995**, *117*, 5534.

(28) Stott, K.; Stonehouse, J.; Keeler, J.; Hwang, T.-L.; Shaka, A. J. *J. Am. Chem. Soc.* **1995**, *117*, 4199.

the *J* data and the molecular mechanics calculations. The observed NOEs are averaged among all the rotamers present in solution. Along this reasoning, it can be observed that the experimental values are in good agreement with those estimated from the MM3* calculated distribution.

All the experimental and theoretical data prove that there are internal motions around the glycosidic linkages.[29] The presence of non-*exo*-anomeric conformers for the glycomimetic is probably smaller than 5%. Thus, the molecular mechanics and NMR results have allowed us to demonstrate the participation of at least two conformers around Φ of the fluoromethylene-linked *C*-disaccharide **1**.[30] The *exo*-anomeric[31] preference for it should mainly reside in steric effects, probably 1,3-type interactions.[5] In fact, for the regular $^4C_1$(D) chairs of the *gluco* series, there is a 1,3-type interaction between the equatorially substituted C-2, as in **1**, and the aglycon when the non-*exo*-anomeric (non-*exo*) conformation is considered (Figure 1). There are not such steric interactions for the *exo*-anomeric (*exo*) and the *anti* conformations. Therefore, this interaction is probably at the origin of the strong preference of the *exo*-anomeric orientation in **1**.[5,31] For *O*-glycosides, the stereoelectronic effect will be additionally superimposed, with a subsequent further stabilization of the *exo*-anomeric orientation, thus providing an explanation for the basically unique conformation around the Φ angle of the *O*-disaccharides.[31] Indeed, MM3* calculations for the *O*-glycosyl analogue **13** point to the major existence of the *syn-exo* conformer (>70%), which corresponds to the minor geometries around Φ of the *C*-disaccharide **1**. Our observation that **1** adopts preferred *anti*-Φ conformations can be interpreted in terms of a stabilizing gauche effect[32] involving the fluorine atom and the ethereal oxygen atom of the glucopyranosyl moiety. Regarding Ψ (rotamers about C1′−C3 bond) of the *O*-glucopyranoside **13**, the calculations predict that the *g*− conformers are highly destabilized and that only the *anti* conformers are possible. The shortening of the C−O bonds with respect to the C−C ones is probably responsible for this fact.

Conclusion

The results presented herein clearly show that the Φ glycosidic linkages (rotation about C1′−C2′ bond) of *C*-glycosyl analogues are more flexible than those of the natural *O*-glycosides, as determined by NMR and molecular mechanics calculations.[33] Our observations with the fluoromethylene-linked *C*-disaccharide **1**, along with those previously obtained for other glycomimetics, are relevant for drug design. The flexibility of these mimetics may limit use them as therapeutic agents: an entropy penalty has to be paid and minima other than the global minimum could be bound by biological receptors.[34] Nevertheless, the small energy barriers between the different energy regions might allow for the global minimum conformation of the glycoside to be bound by a protein without a major energy conflict. In addition, these compounds may be excellent probes to study the combining sites of proteins and enzymes and they may also serve as test compounds to compare conformational properties of oligosaccharides.[35,36] Our work suggests that stereospecific monofluorination of the methylene linker of a *C*-glycoside can be used to favor "unnatural" conformations of the glycomimetic.

Experimental Section

General Remarks. See ref 37. None of the procedures were optimized. Flash column chromatography (FC) was performed on Merk silica gel (230−400 mesh). Thin-layer chromatography (TLC) was carried out on silica gel (Merk aluminum foils).

NMR Spectroscopy. ^{1}H NMR signal assignments were confirmed by double irradiation experiments and, when required, by 2D-NOESY and COSY spectra. *J* values are given in hertz. The 600 MHz ^{1}H NMR spectra were recorded on a Bruker AMX-600 FR spectrometer. The 500 MHz ^{1}H NMR spectra in D_2O were recorded on a Varian Unity 500 spectrometer, using an approximately 2 mg/mL solution at different temperatures (299−313 K). Chemical shifts are reported in ppm, using external TMS (0 ppm) as reference. The double quantum filtered COSY spectrum was performed with a data matrix of 256 × 1K to digitize a spectral width of 2000 Hz. A total of 16 scans were used with a relaxation delay of 1 s. The 2D TOCSY esperiment was performed using a data matrix of 256 × 2K to digitize a spectral width of 2000 Hz; 4 scans were used per increment with a relaxation delay of 2 s. MLEV 17 was used for the 100 ms isotropic mixing time. The one-bond proton−carbon correlation experiment was collected in the ^{1}H-detection mode using the HSQC sequence and a reverse probe. A data matrix was used to digitize a spectral width of 2000 Hz in F_2 and 10000 Hz in F_1; 4 scans were used per increment with a relaxation delay of 1 s and a delay corresponding to a *J* value of 145 Hz. A BIRD pulse was used to minimize the proton signals bonded to ^{12}C. ^{13}C decoupling was achieved by the WALTZ scheme.

NOESY experiments were performed with the selective 1D double pulse field gradient spin echo module, using three different mixing times, namely, 250, 500, and 750 ms. 2D NOESY experiments were also performed with the same mixing times and using 256 × 2K matrixes.

NOE Calculations. NOESY spectra were simulated according to a complete relaxation matrix approach, following the protocol previously described, using three different mixing times (between 250 and 750 ms). The spectra were simulated

(29) For a detailed description of conformational analysis of carbohydrates using MD simulations, see: Woods, R. J. *Curr. Opin. Struct. Biol.* **1995**, *5*, 591.

(30) Neuhaus, D.; Williamson, M. P. *The Nuclear Overhauser Effect in Structural and Conformational Analysis;* VCH Publishers: New York, 1989.

(31) (a) Lemieux, R. U.; Koto, S.; Voisin, D. *Am. Chem. Soc. Symp. Ser.* **1979**, *87*, 17. (b) Thatcher, G. R. J. *The Anomeric Effect and Associated Stereoelectronic Effects*; American Chemical Society: Washington, DC, 1993. (c) Tvaroska, I.; Bleha, T. *Adv. Carbohydr. Chem. Biochem.* **1989**, *47*, 45. (d) Kirby, A. J. *The Anomeric Effect and Related Stereoelectronic Effects at Oxygen*; Springer-Verlag: Heidelberg, Germany, 1983.

(32) (a) Allen, L. C. *Chem. Phys. Lett.* **1968**, *2*, 597. (b) Wolfe, S. *Acc. Chem. Res.* **1972**, *5*, 102. (c) Olson, W. K. *J. Am. Chem. Soc.* **1982**, *104*, 278. (d) Wiberg, K. B.; Murko, M. A.; Laidig, K. E.; MacDougall, P. J. *J. Phys. Chem.* **1990**, *94*, 6956. (e) Thibaudeau, C.; Plavec, J.; Garg, N.; Papchikhin, A.; Chattopadhyaya, J. *J. Am. Chem. Soc.* **1994**, *116*, 4038. (f) Bakke, J. M.; Bjerkeseth, L. H.; Ronnow, T. E. C. L.; Steinsvoll, K. *J. Mol. Struct.* **1994**, *321*, 205. (g) Abraham, R. J.; Chambers, E. J.; Thomas, W. A. *J. Chem. Soc., Perkin Trans. 2* **1994**, 949. (h) Rablen, P. R.; Hoffmann, R. W.; Hrovat, D. A.; Borden, W. T. *J. Chem. Soc., Perkin Trans. 2* **1999**, 1719.

(33) Poveda, A.; Asensio, J. L.; Bazin, H.; Polat, T.; Lindhardt, R. J.; Jimenez-Barbero, J. *Eur. J. Org. Chem.* **2000**, 1805.

(34) For different implications of conformational restriction of the ligand upon protein binding, see: Bundle, D. R.; Alibés, R.; Nilar, S.; Otter, A.; Warwas, M.; Zhang, P. *J. Am. Chem. Soc.* **1998**, *120*, 5317.

(35) For a different conclusion, see: Navarre, N.; Amiot, N.; Van Oijen, A. H.; Imberty, A.; Poveda, A.; Jimenez-Barbero, J.; Cooper, A.; Nutley, M. A.; Boons, G. J. *Chem. Eur. J.* **1999**, *5*, 2281.

(36) For conformational selection in carbohydrate recognition by proteins, see refs 9−12 and Gilleron, M.; Siebert, H.-C.; Kaltner, H.; Von der Lieth, C. W.; Kozar, T.; Halkes, K. M.; Korchagina, E. Y.; Bovin, N. V.; Gabius, H.-J.; Vliegenthart, J. F. G. *Eur. J. Biochem.* **1998**, *249*, 27.

(37) (a) Sevin, A. F.; Vogel, P. *J. Org. Chem.* **1994**, *59*, 5920. (b) Kraehenbuehl, K.; Picasso, S.; Vogel, P. *Helv. Chim. Acta* **1998**, *81*, 1439.

from the average distances $\langle r^{-6}\rangle_{kl}$ calculated from the population distribution at 303 K. Isotropic motion and external relaxation of 0.1 s^{-1} were assumed. A τ_c of 50 ps was used to obtained the best match between experimental and calculated NOEs for the intraresidue proton pairs (Fuc H1/H2). All NOE calculations were automatically performed by a homemade program, available from the authors upon request.

Molecular Mechanics and Dynamics Calculations. Molecular mechanics and dynamics calculations were performed using the MM3* force field as implemented in MACROMODEL 4.5. Glycosidic torsion angles are defined as Φ (H2′−C2′/C1′−C3), Ψ (C2′−C1′/C3−C4), ω1 as (O4−C4/C5−C6), ω2 as (C4−C5/C6−O6), and ω3 as (C5′−C6′/C7′−O). The results are shown in Table 1. For Ψ and ω, the rotamers are defined as *g*+ (60°), g− (−60°), and *anti* (180°), while for Φ, conformers in agreement with the *exo*-anomeric orientation (Φ ca. +60) and in disagreement (Φ ca. −60) are denoted as *exo* and non-*exo*, respectively. The dielectric constant $\epsilon = 80$ and the continuum GB/SA solvent model were performed. Eighty-one initial geometries were considered, by combining the stagerred orientations for Φ, Ψ, and ω. From the energy values, probability distributions were calculated for each conformer, according to a Boltzmann function at 300 K.

The global energy minimum structure was used as starting geometry for molecular dynamics (MD) simulations at 300 K, with the GB/SA solvent model and a time step of 1 fs. The equilibration period was 100 ps. After this period, structures were saved every 0.5 ps. The total simulation time was 3 ns. Average distances between intraresidue and interresidue proton pairs were calculated from the dynamics simulations.

1,6:2,3-Dianhydro-3-*C*-[(1*R*)-2,6-anhydro-3,4,5,7-tetra-*O*-benzyl-1-deoxy-1-fluoro-D-*glycero*-D-*gulo*-heptitol-1-*C*-yl]-*β*-D-*ribo*-hex-4-ulopyranose ((+)-6). A solution of (+)-**5**[18] (1.61 g, 2.3 mmol) in CH_2Cl_2 (30 mL) was added to a stirred solution of DAST (0.84 mL, 6.4 mmol) in CH_2Cl_2 (30 mL) cooled to −95 °C. The reaction mixture was allowed to warm to room temperature overnight. Then H_2O (50 mL) was added. The aqueous layer was extracted with CH_2Cl_2 (50 mL, 3 times). The combined organic extracts were washed with brine (50 mL) and dried ($MgSO_4$). Solvent evaporation and flash chromatography on silica gel (3:1 light petroleum ether/EtOAc) afforded 1.17 g (73%) of a white solid which was crystallized (4:1 hexane/EtOAc): mp 91 °C; $[\alpha]^{25}_D = +5.3$ ($c = 0.22$, $CHCl_3$); ^{1}H NMR (400 MHz, $CDCl_3$) δ 7.33−7.09 (m, 20H), 5.46 (br s, 1H), 5.03 (dd, $J = 44.0$, 2.6, 1H), 4.8−4.51 (m, 6H), 4.40−4.38 (m, 3H), 3.86 (dd, $J = 8.6$, 1.6, 1H), 3.72 (ddd, $J = 17.0$, 9.3, 2.6, 1H), 3.68 (dd, $J = 10.7$, 2.9, 1H), 3.63−3.55 (m, 5H), 3.39 (br s, 1H), 3.27 (m, $J = 9.3$, 1H).

1,6:2,3-Dianhydro-3-*C*-[(1*R*)-2,6-anhydro-3,4,5,7-tetra-*O*-benzyl-1-deoxy-1-fluoro-D-*glycero*-D-*gulo*-heptitol-1-*C*-yl]-*β*-D-*gulo*-pyranose ((+)-8). $NaBH_4$ (96 mg, 2.6 mmol) was added portionwise to a stirred solution of (+)-**6** (1.1 g, 1.6 mmol) in MeOH (40 mL) cooled to 0 °C. After stirring at 0 °C for 2 h, CH_2Cl_2 (50 mL), H_2O (50 mL), and 1 M aqueous HCl (5 mL) were added. The aqueous layer was extracted with CH_2Cl_2 (50 mL, 3 times), and the combined organic extracts were washed with brine (50 mL) and dried ($MgSO_4$). Solvent evaporation afforded 1.1 g (100%) of a white solid pure enough for the next steps: mp 38 °C; $[\alpha]^{25}_D = +23$ ($c = 0.24$, $CHCl_3$); ^{1}H NMR (400 MHz, $CDCl_3$) δ 7.36−7.13 (m, 20H), 5.55 (br s, 1H), 5.07 (dd, $J = 45.0$, 8.2, 1H), 4.85−4.67 (m, 5H), 4.47−4.41 (m, 3H), 4.28 (ddd, $J = 6.3$, 4.5, 1.8, 1H), 4.14 (d, $J = 4.5$, 1H), 4.08 (dd, $J = 8.2$, 1.8, 1H), 3.86−3.53 (m, 8H), 3.24 (s, 1H).

1,6:2,3-Dianhydro-3-*C*-[(1*R*)-2,6-anhydro-1-deoxy-1-fluoro-D-*glycero*-D-*gulo*-heptitol-1-*C*-yl]-*β*-D-*gulo*-pyranose ((+)-9). Metallic Na (1 g, 43 mmol) was added to liquid NH_3 (30 mL, condensed at −78 °C). A solution of (+)-**8** (1.07 g, 1.5 mmol) in anhydrous THF (12 mL) was added dropwise with stirring. After stirring at −78 °C for 50 min, solid NH_4Cl (4 g) was added and the cooling bath removed. Once at 20 °C, the residue was taken up in MeOH and purified by flash chromatography on silica gel (3:1 CH_2Cl_2/MeOH), affording 0.5 g (95%) of a hygroscopic white solid: $[\alpha]^{25}_D = +5.6$ ($c = 0.45$, MeOH); ^{1}H NMR (400 MHz, CD_3OD) δ 5.57 (br s, 1H), 4.97 (dd, $J =$ 47.0, 5.0, 1H), 4.35 (ddd, $J = 6.2$, 5.1, 1.8, 1H), 4.24 (d, $J =$ 5.1, 1H), 4.18 (dd, $J = 8.1$, 1.8, 1H), 3.88 (dd, $J = 12.1$, 2.1, 1H), 3.79−3.71 (m, 3H), 3.48 (dd, $J = 8.9$, 8.8, 1H), 3.41 (dd, $J = 8.9$, 8.85, 1H), 3.36 (dd, $J = 8.9$, 8.85, 1H), 3.33 (m, 1H), 3.25 (dd, $J = 1.2$, 1.1, 1H).

4-*O*-Acetyl-1,6:2,3-dianhydro-3-*C*-[(1*R*)-3,4,5,7-tetra-*O*-acetyl-2,6-anhydro-1-deoxy-1-fluoro-D-*glycero*-D-*gulo*-heptitol-1-*C*-yl]-*β*-D-*gulo*-pyranose ((+)-10). A mixture of (+)-**9** (480 mg, 1.42 mmol), Ac_2O (5.4 mL), pyridine (9 mL), and 4-(dimethylamino)pyridine (0.5 mg) was stirred at 20 °C for 15 h. Solvent evaporation in vacuo gave a residue that was taken up in toluene (10 mL), and the solvent was evaporated to dryness in vacuo. The latter operation was repeated and the residue purified by flash chromatography on silica gel (1:2 light petroleum ether/EtOAc), affording 751 mg (96%) of a white solid: mp 63 °C; $[\alpha]^{25}_D = +32$ ($c = 0.08$, $CHCl_3$); ^{1}H NMR (400 MHz, $CDCl_3$) δ 5.62 (s, 1H), 5.24 (dd, $J = 9.3$, 9.25, 1H), 5.22 (d, $J = 4.7$, 1H), 5.16 (dd, $J = 9.3$, 9.25, 1H), 5.04 (dd, $J = 45.0$, 7.8, 1H), 5.00 (dd, $J = 9.3$, 9.25, 1H), 4.51 (ddd, $J =$ 6.3, 4.7, 1.7, 1H), 4.17, (dd, $J = 12.6$, 5.2, 1H), 4.05 (dd, $J =$ 12.6, 5.2, 1H), 3.99 (dd, $J = 8.3$, 1.7, 1H), 3.79−3.70 (m, 3H), 3.29 (s, 1H), 2.13, 2.10, 2.03, 2.02, 2.01 (5s, 15H).

1,4,6-Tri-*O*-acetyl-2,3-anhydro-3-*C*-[(1*R*)-3,4,5,7-tetra-*O*-acetyl-2,6-anhydro-1-deoxy-1-fluoro-D-*glycero*-D-*gulo*-heptitol-1-*C*-yl]-α-D-*gulo*-pyranose ((+)-11). A mixture of (+)-**10** (387 mg, 0.71 mmol), Ac_2O (3 mL), and CF_3COOH (2 mL) was stirred at 20 °C for 2.5 h. It was poured into ice (10 mL) and neutralized with a saturated aqueous solution of $NaHCO_3$ (pH 8). The mixture was extracted with EtOAc (10 mL, 3 times). The combined organic extracts were washed with brine (30 mL) and dried ($MgSO_4$). Solvent evaporation and flash chromatography on silica gel (1:2 light petroleum ether/EtOAc) afforded 336 mg (73%) of a white solid: mp 137 °C; $[\alpha]^{25}_D = +16$ ($c = 0.08$, $CHCl_3$); ^{1}H NMR (400 MHz, $CDCl_3$) δ 6.34 (d, $J = 3.0$, 1H), 5.55 (br s, 1H), 5.25−5.18 (m, 2H), 5.04 (dd, $J = 9.5$, 9.45, 1H), 4.72 (dd, $J = 46.0$, 6.7, 1H), 4.27 (dd, $J = 12.4$, 2.2, 1H), 4.25 (ddd, $J = 7.2$, 5.5, 1.4, 1H), 4.09 (dd, $J = 11.6$, 5.5, 1H), 4.08, (dd, $J = 12.4$, 5.5, 1H), 3.93, (dd, $J =$ 11.6, 7.2, 1H), 3.77 (m, 1H), 3.75 (d, $J = 3.0$, 1H), 3.71 (ddd, J = 9.5, 5.5, 2.2, 1H), 2.18, 2.15, 2.11, 2.05, 2.045, 2.02, 2.015 (7s, 21H).

7:1 Mixture of 2,3-Anhydro-3-*C*-[(1*R*)-2,6-anhydro-1-deoxy-1-fluoro-D-*glycero*-D-*gulo*-heptitol-1-*C*-yl]-*β*-D-*gulo*-furanose (1) and 2,3-Anhydro-3-*C*-[(1*R*)-2,6-anhydro-1-deoxy-1-fluoro-D-*glycero*-D-*gulo*-heptitol-1-*C*-yl]-*β*-D-*gulo*-pyranose (12). A mixture of (+)-**11** (97 mg, 0.15 mmol) and a saturated solution of NH_3 in MeOH (7 mL) was stirred at 20 °C for 3.5 h. Solvent evaporation in vacuo afforded pure **1**, **12**, and acetamide (by ^{1}H NMR). Chromatography on silica gel (1.7:1 $CHCl_3$/MeOH) afforded 38 mg (72%) of a 7:1 mixture of **1** and **12** as a hygroscopic white solid: $[\alpha]^{25}_D = -7.4$ ($c = 0.15$, MeOH); ^{1}H NMR (600 MHz, CD_3OD) of **1**, δ 5.34 (d, $J = 2.8$, 1H), 4.83 (dd, $J = 46.0$, 4.2, 1H), 4.70 (d, $J = 2.4$, 1H), 4.12 (br.d, $J = 2.4$, 1H), 3.88 (dd, $J = 12.3$, 2.2, 1H), 3.75 (ddd, $J =$ 13.0, 9.4, 4.2, 1H), 3.72 (d, $J = 2.8$, 1H), 3.68 (dd, $J = 12.3$, 5.6, 1H), 3.66−3.62 (m, 2H), 3.51 (dd, $J = 9.4$, 9.35, 1H), 3.41 (dd, $J = 9.4$, 9.35, 1H), 3.36 (dd, $J = 9.45$, 9.4, 1H), 3.28 (dd, $J = 9.45$, 5.6, 2.2, 1H); ^{19}F NMR (376.4 MHz, CD_3OD) of **1**, δ −193.0 (dd, $J = 46.0$, 13.0, 1F); ^{13}C NMR (100.6 MHz, CD_3-OD) of **1**, δ 95.5 (d, ^1J(C,H) = 173), 94.2 (dd, ^1J(C,F) = 174, ^1J(C,H) = 155), 82.2 (d, ^1J(C,H) = 142), 79.9 (dd, ^1J(C,H) = 142, ^2J(C,F) = 21), 79.6 (d, ^1J(C,H) = 143), 75.6 (d, ^1J(C,H) = 148), 72.9 (dd, ^1J(C,H) = 145, ^3J(C,F) = 5), 72.1 (d, ^1J(C,H) = 144), 71.2 (d, ^1J(C,H) = 145), 64.2 (t, ^1J(C,H) = 142), 63.6 (d, ^2J(C,F) = 26), 62.7 (t, ^1J(C,H) = 141), 61.3 (dd, ^1J(C,H) = 193, ^3J(C,F) = 6).

X-ray Crystal Structure Analysis. Crystallographic data (excluding structure factors) for 1,6:2,3-dianhydro-3-*C*-[(1*R*)-2,6-anhydro-3,4,5,7-tetra-*O*-benzyl-1-deoxy-1-fluoro-D-*glycero*-D-*gulo*-heptitol-1-*C*-yl]-*β*-D-*ribo*-pyranose (**7**, hydrate of (+)-**6**) have been deposited with the Cambridge Data Centre as supplementary publication under no. CCDC. 155696. Copies of these data can be obtained free of charge on application to CCDC, 12 Union Road, Cambridge CB21EZ, UK (fax: +41 1223 336033; e-mail: deposit@ccdc.cam.ac.uk).

Acknowledgment. We thank the Swiss National Science Foundation, the Fonds Herbette (Lausanne), the Office Fédéral de l'Enseignement et de la Science (Bern, european COST D13/0001/99 action), and the DGICYT (Madrid, grant BQU2000-1501-C02-01) for financial support. We thank also Mr. Martial Rey and Franscisco Sepúlveda for technical help.

Supporting Information Available: Detailed ^{1}H and ^{13}C NMR spectra and signal assignments, further rotations data, and UV, IR, and MS spectra; ^{1}H NMR NOESY, ^{1}H NMR DPFGNOE, and ^{1}H NMR TOCSY spectra of **1**; ORTEP representation of **7**; superimposition of 100 snapshots from one of the MD simulations for **1**. This material is available free of charge via the Internet at http://pubs.acs.org.

JO0102462